Numerical method for assessing the potential of smart engine thermal management: application to a medium-upper segment passenger car

F. Caresana, M. Bilancia, C.M. Bartolini

Accepted Manuscript

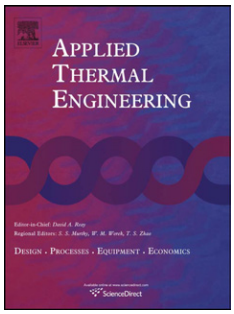

Title: Numerical method for assessing the potential of smart engine thermal management: application to a medium-upper segment passenger car

Authors: F. Caresana, M. Bilancia, C.M. Bartolini

PII: S1359-4311(11)00374-7

DOI: 10.1016/j.applthermaleng.2011.07.017

Reference: ATE 3644

To appear in: *Applied Thermal Engineering*

Received Date: 6 July 2010

Revised Date: 24 May 2011

Accepted Date: 10 July 2011

Please cite this article as: F. Caresana, M. Bilancia, C.M. Bartolini. Numerical method for assessing the potential of smart engine thermal management: application to a medium-upper segment passenger car, Applied Thermal Engineering (2011), doi: 10.1016/j.applthermaleng.2011.07.017

Numerical method for assessing the potential of smart engine thermal management: application to a medium-upper segment passenger car

F. Caresana[a*], M. Bilancia[b], C.M. Bartolini[c]

[a]Università Politecnica delle Marche
Dipartimento di Energetica, Via Brecce Bianche, 60131 Ancona (ITALY)

[b]General Motors Powertrain Europe Srl
Corso Castelfidardo, 36, 10128 Torino (ITALY)

[c]Università degli Studi e-Campus
Via Isimbardi 10, 22060 Novedrate (ITALY)

*Corresponding author: Tel.(+39) 071 2204 765, Fax (+39) 071 2204 770,
email: f.caresana@univpm.it

ABSTRACT

Significant reductions in vehicle fuel consumption can be obtained through a greater control of the thermal status of the engine, especially under partial load conditions. Different systems have been proposed to implement this concept, referred to as improved engine thermal management. The amount of fuel saved depends on the components and layout of the engine cooling plant and on the performance of its control system. In this work, a method was developed to calculate the theoretical minimum fuel consumption of a passenger car and used as a reference in comparing different engine cooling system concepts. A high-medium class car was taken as an example and simulated on standard cycles. Models for power train and cooling system components were developed and linked to simulate the vehicle. A preliminary analysis of the engine was performed using AVL's Boost program. The fuel consumption of the complete vehicle, equipped with a conventional cooling plant, was determined on standard cycles and compared with that of a vehicle equipped with a 'perfect' cooling system, to calculate the theoretical reduction in fuel consumption.

Keywords

Engine thermal management, cooling system, fuel consumption reduction, heat transfer coefficient, nucleate boiling

NOMENCLATURE

A_a	heat transfer area between engine block and air (m^2)
A_{eb}	heat transfer area between coolant and engine block (m^2)
A_l	heat transfer area between liner and coolant (m^2)
A_r	radiator heat transfer area (external) (m^2)
B	cylinder bore (m)
BMEP	brake mean effective pressure (Pa) ,(bar)
c_c	coolant specific heat capacity ($J\ kg^{-1}\ K^{-1}$)
c_{eb}	engine block specific heat capacity ($J\ kg^{-1}\ K^{-1}$)
c_l	liner specific heat capacity ($J\ kg^{-1}\ K^{-1}$)
c_{oil}	oil specific heat capacity ($J\ kg^{-1}\ K^{-1}$)
FMEP	engine friction mean effective pressure (Pa) ,(bar)
h_{eboil}	liner height at which liner temperature equals coolant boiling temperature (m)
h_l	liner height (m)
l_t	normalized thermostatic valve lift (-)
$m_{c,e}$	mass of coolant in the engine (kg)
$m_{c,r}$	mass of coolant in the radiator (kg)
m_{eb}	engine block mass (kg)
$\dot{m}_f$	fuel consumption ($g\ s^{-1}$)

m_l	liner mass (kg)
m_{oil}	oil mass (kg)
$\dot{m}_a$	air mass flow through the radiator ($kg\ s^{-1}$)
$\dot{m}_{by}$	coolant mass flow through the by-pass duct ($kg\ s^{-1}$)
$\dot{m}_c$	coolant mass flow through the engine ($kg\ s^{-1}$)
$\dot{m}_r$	coolant mass flow through the radiator ($kg\ s^{-1}$)
n_e	engine rotational speed (min^{-1})
Pr	Prandtl number (-)
$\dot{Q}_a$	engine block to air heat transfer rate (W)
$\dot{Q}_{eb}$	coolant to engine block heat transfer rate (W)
$\dot{Q}_f$	heat transfer rate due to friction (W)
$\dot{Q}_{gw}$	gas to liner heat transfer rate (W)
$\dot{Q}_r$	coolant to air heat transfer rate in the radiator (W)
$\dot{Q}_{wc}$	liner to coolant heat transfer rate (W)
Re	Reynolds number (-)
S	piston stroke (m)
T_a	cooling air temperature (K)
T_{boil}	coolant boiling temperature (K)
$T_{c,\,e\_in}$	coolant temperature at engine inlet (K)
$T_{c,\,e\_out}$	coolant temperature at engine outlet (K)
$T_{c,\,r\_out}$	coolant temperature at radiator outlet (K)
T_e	mean actual engine temperature (K)
T_{eb}	engine block temperature (K)
T_l	liner temperature (K)
T_w	mean liner temperature (K)
T_∞	fully warmed up engine temperature (K)
V	engine displacement (m^3)
v_a	air velocity through the radiator ($m\ s^{-1}$)
α_a	engine block to air heat transfer coefficient ($W\ m^{-2}\ K^{-1}$)
α_{eb}	coolant to engine block heat transfer coefficient ($W\ m^{-2}\ K^{-1}$)
α_r	coolant to air heat transfer coefficient ($W\ m^{-2}\ K^{-1}$)
α_{wc}	wall to coolant heat transfer coefficient ($W\ m^{-2}\ K^{-1}$)
ε	engine revs per cycle ($rad\ s^{-1}$)
λ_c	coolant thermal conductivity ($W\ m^{-1}\ K^{-1}$)
τ	engine to wheel transmission ratio (-)
ω_e	engine angular speed ($rad\ s^{-1}$)
Γ_t	tyre circumference (m)

1. INTRODUCTION

The heat dissipation capacity of conventional engine cooling systems is designed for maximum power operating conditions. However, since vehicle engines most often operate under partial load conditions, such systems are in fact

oversized, entailing unnecessary heat losses, mechanical losses, as well as parasitic losses from high rotational speed operation of the mechanical components.

Adapting the cooling system to variable operating conditions can effectively reduce fuel consumption (thus curbing harmful emissions) as well as improve engine efficiency. Several advanced automotive cooling systems have been devised to achieve this goal. Most entail replacing the standard wax thermostat valve, mechanical water pump and radiator fan with a variable position smart valve, a variable-speed electrical pump and a variable-speed radiator fan. Engine over- and under-cooling are easily managed by controlling the coolant mass flow through engine and radiator via smart valve position and/or pump speed. The enabling technology to exploit their potential is offered by computer control.

Dynamic models for the thermal system, smart thermostat valve, coolant pump, and radiator fan have been described in [1], where the cooling system configuration has been tested by replacing the engine with an electronic immersion heater and by operating the actuators via a non-linear tracking controller. Enhancement of gasoline and diesel engine thermal management systems through a smart thermostat valve and a variable speed water pump has been discussed in [2], where a non-linear tracking controller has been proposed to ensure that engine temperature follows the desired trajectory. A non-linear controller has also been designed for transient temperature tracking in an experimental system involving a variable position smart valve, a variable speed electrical water pump, a variable speed electrical radiator fan, an engine block, and various sensors [3]; in this system a steam-based heat exchanger mimics the heat generated by the engine's combustion process. The power consumption associated with four different simulated solutions has been compared in a comprehensive assessment of different configurations for a heavy-duty diesel engine [4].

Since pure electrical solutions involve greater electricity consumption, which raise serious problems with standard low-voltage power circuits [4, 5], hydraulic-driven actuators have also been proposed [e.g. 6].

Although the main goals of an improved thermal management system are greater engine efficiency and a reduction of harmful emissions, the typically faster engine heating and higher engine temperature of automotive applications result in greater comfort and safety in winter (better cabin climate control and faster windshield defrosting) [7].

The advantages of using a smart thermal management system have also been investigated by modelling the system by means of 1-D simulation packages. Of the several commercial software packages designed for modelling an automotive cooling system most use a 1-D lumped parameter approach. Tumus et al [8] employed this approach to develop a thermal management system modelling tool. In some studies the components have not been physically built or tested, and mathematical models have been constructed to model theoretical systems (e.g. [9], [10] and [11]).

Shortening the engine starting and warm-up time can be crucial to meeting new requirements and regulations, since these phases involve the greatest fuel consumption and pollutant emissions. These questions were addressed in [12], which modelled the basic engine cooling system and then simulated and compared various design options.

The works cited above demonstrate experimentally or simulate the benefits of flexible control cooling systems only in particular configurations. We opted against addressing a particular arrangement; instead, we decided to focus on a question that published data leave unanswered: the maximum fuel economy that can be achieved by fitting a smart thermal management system in a car. The answer should be obtained from comparisons between conventional and smart cooling systems in standard tests and would depend on the class of the car, the test cycle chosen as the reference, and on 'how smart' the cooling system was. Result generalization would require analyzing data for different classes of cars and different cooling system concepts; however, the field is too new and the task too daunting to be accomplished by a single research group. Besides, obtaining such results experimentally would be quite difficult and expensive. Our contribution to answering the question is therefore through the development of a method based on numerical simulation, which we then tested in an upper-medium segment passenger car.

The method is based on defining a 'perfect' cooling system, whose performance is then used as a benchmark to which different concepts can be compared. AVL's Boost program, a well-tested commercial tool, was used to simulate the engine's thermal and mechanical behaviour, then a code was developed in Matlab-Simulink incorporating the Boost results and the models for the cooling system, the drive train and the vehicle aerodynamics.

The main concepts behind the paper are outlined in section 2, where a 'perfect' cooling system is defined. The theoretical aspects and the methods used to solve individual problems are then described in sections 3 and 4; in particular, section 3.1 deals with engine simulation, section 3.2 with the cooling system models, and section 3.3 with the vehicle characteristics and driving cycle simulator. Section 4 reports some examples of the results that can be obtained using the proposed method; finally, the conclusions are drawn in section 5.

2. THE "PERFECT" COOLING SYSTEM

The fuel economy that can be achieved in a vehicle powered by an internal combustion engine using a smart thermal management system depends on the cooling system's layout, component type and performance, and control technique. Since different arrangements may involve quite different fuel consumption performances in relation to different complexity and cost, it would be useful to know how distant a particular solution is from the optimum. This can be done by defining the performance of a perfect cooling system to which different concepts of smart cooling can then be compared.

Accordingly, the first aim of this paper was to define the characteristics of such perfect cooling system and use it as a benchmark to evaluate the fuel economy potential of a smart thermal management.

A perfect cooling system is one devoid of defects, something that cannot be obtained in practice; this system was therefore used as a reference.

2.1 Definition of the perfect cooling system

A perfect cooling system is one that meets the following three principles (principle #3a may be an alternative to #3):

1) it is able to maintain the engine constantly at its set point temperature
2) it does not require additional energy for component functioning with respect to a conventional system
3) it is able to warm-up the engine instantly

3a) during the warm-up phase the system is adiabatic.

Principle #1 entails a perfect control system.
Principle #2 allows neglecting the performance details of the cooling system components at this stage of the work; in fact, a reduction of the energy required for engine cooling can be assumed to be a consequence, for example, of the use of more efficient pumps or pumping strategies, but since many concepts also involve substitution of mechanical with electrical components, the gain is not guaranteed and is system-dependent.
Principles #3 and #3a make reference to the engine's warm-up which, together with efficiency and fuel combustion, is very important for pollutant emissions. Shortening the warm-up time has been proved to reduce emissions.
Besides the mass and the thermal characteristics of the engine itself and the engine CPU strategy, the warm-up time depends on the amount of cooling fluid contained in the plant, on its flow rate, and on the system's thermal insulation. In fact, part of the heat generated during warm-up is transferred to the cooling fluid and part is dissipated to the ambient through the engine walls and the cooling system components.
Since principle #3 is impracticable, the more realistic principle #3a was tested as an alternative. The data obtained by applying principle #3 quantify the system's performance without taking into consideration the effect of the warm-up transient. Differences in performance related to principles #3 and #3a allow highlighting the influence of the warm-up phase.

3. ENGINE AND COOLING SYSTEM THERMAL MODELLING

3.1. Engine model

To analyze how the cooling system design affects engine performance, a four-stroke, four-cylinder, naturally aspirated gasoline engine was simulated using AVL's Boost program. The engine's main technical data are reported in table 1. The Boost diagram and the simulated performances of the engine in Wide Open Throttle (WOT) condition are shown in figure 1.
Complete engine behaviour simulations were run at different thermal levels, ranging from cold to fully warmed up. In the Boost program the different thermal levels were simulated by taking different values for the liner mean temperature T_w , which for the present engine ranges from 107°C (fully warmed up) to 25°C (cold).
For each thermal level the simulations consisted in running the code at different degrees of throttle valve opening, from minimum to WOT, and for each throttle position at different rotational speeds, from minimum to maximum, by 250 rpm increases.
The Boost program's output data were then post-processed to obtain maps of engine fuel consumption, $\dot{m}_f$, and of the heat transfer rate between combustion gases and engine walls, $\dot{Q}_{gw}$, as a function of brake mean effective pressure (*BMEP*) and engine rotational speed. The latter information on the thermal behaviour of the engine would have been particularly difficult to obtain via an experimental approach.
As examples of the results, figures 2 and 3 show the engine rotational speed–*MEP* charts and the iso-$\dot{m}_f$ and iso-$\dot{Q}_{gw}$ curves for the cold and the fully warmed up engine. Figure 2 also reports the engine working points for the European City driving cycle (EU CITY) and the New European Driving Cycle (NEDC) (see section 4 for vehicle details).
At any given working point, with the engine cold, fuel consumption is significantly greater (figure 2) and the combustion gases transfer to the walls a larger amount of heat per unit time (figure 3).

3.2. Cooling system model

This section deals with the thermo-fluid-dynamic models for internal and external engine cooling systems, which are described in sections 3.2.1 and 3.2.2, respectively. The coolant is assumed to exchange heat only in the radiator and the engine; all the other components are assumed to be adiabatic in the model.

3.2.1 Internal cooling system

The internal cooling system consists of the coolant paths in the engine. Three main components were considered as parts of the internal cooling system: the liner, the coolant and the engine block (see figure 4). Accordingly, three enthalpy balances were formulated using a lumped parameter approach:
Enthalpy balance for the liner:

$$\dot{Q}_{gw} - \dot{Q}_{wc} = m_l \cdot c_l \cdot \frac{dT_w}{dt} \quad (1)$$

Enthalpy balance for the coolant:

$$\dot{Q}_{wc} + \dot{m}_c \cdot c_c \cdot T_{c,e\_in} - \dot{m}_c \cdot c_c \cdot T_{c,e\_out} - \dot{Q}_{eb} = m_{c,e} \cdot c_c \cdot \frac{dT_{c,e\_out}}{dt} \quad (2)$$

Enthalpy balance for the engine block, whose temperature is assumed to be the same as the oil's:

$$\dot{Q}_{eb} + \dot{Q}_f - \dot{Q}_a = (m_{eb} \cdot c_{eb} + m_{oil} \cdot c_{oil}) \cdot \frac{dT_{eb}}{dt} \quad (3)$$

The heat transfer rates from liner walls to coolant, $\dot{Q}_{wc}$, from coolant to engine block, $\dot{Q}_{eb}$, and from coolant to ambient air, $\dot{Q}_a$, were calculated using the following relationships:

$$\dot{Q}_{wc} = \alpha_{wc} \cdot A_l \cdot \left(T_w - \frac{T_{c\_out} + T_{c\_in}}{2} \right) \quad (4)$$

$$\dot{Q}_{eb} = \alpha_{eb} \cdot A_{eb} \cdot \left(\frac{T_{c\_out} + T_{c\_in}}{2} - T_{eb} \right) \quad (5)$$

$$\dot{Q}_a = \alpha_a \cdot A_a \cdot (T_{eb} - T_a) \quad (6)$$

The coolant to engine block heat transfer coefficient, α_{eb}, was obtained using the Dittus-Boelter correlation (eq. A. 1 in the appendix) [12].
The engine block to air heat transfer coefficient was calculated using the correlation [12]:

$$\alpha_a = 0.036 \cdot \mathrm{Pr}^{1/3} \cdot \mathrm{Re}^{0.8} \left(\frac{L_{eb}}{\lambda_a} \right) \quad (7)$$

Prandtl's and Reynolds' numbers in equation (7) regard the air flowing around the engine block, calculated for ambient conditions; its velocity was calculated by reducing vehicle speed by a factor that accounted for engine compartment geometry.
Evaluation of the heat transfer coefficient between engine walls and coolant, α_{wc}, is complicated by the fact that at high engine loads the engine wall temperature in some regions may be higher than the coolant boiling temperature. In such conditions nucleate boiling may occur, and use of correlations that take into account only liquids would result in significant errors.
The details of the procedure used to calculate α_{wc} are reported below in section 3.2.1.1.
$\dot{Q}_f$ in (3) represents the heat transfer rate due to mechanical friction, and can be obtained from the engine Friction Mean Effective Pressure (*FMEP*):

$$\dot{Q}_f = FMEP \cdot V \cdot \frac{\omega_e}{\varepsilon} \quad (8)$$

FMEP in (8) was evaluated by means of the ETH friction model relationship [7]:

$$FMEP = \chi(T_e) \cdot k_1(T_\infty) \cdot (k_2 + k_3 \cdot S^2 \cdot \omega_e{}^2) \cdot \prod \cdot \sqrt{\frac{k_4}{B}} \quad (9)$$

In (9) the engine thermal condition is taken into account through term $\chi(T_e) = \frac{k_1(T_e)}{k_1(T_\infty)}$, whose diagram is reported in figure 5 as a function of the difference between maximum engine temperature, T_∞, and actual engine temperature, T_e.
The values for the coefficients used in (9) are:

$$k_1(T_\infty) = 3 \cdot 10^5 [Pa] \;;\; k_2 = 0.6 \;;\; k_3 = 2.6 \cdot 10^{-4} [s^2/m^2] \;;\; k_4 = 0.029 [m] \;;\; \prod = 1$$

3.2.1.1 Wall to coolant heat transfer coefficient

As noted above, evaluation of the heat transfer coefficient between engine walls and coolant , α_{wc} , is complicated by the fact that at high engine loads the engine wall temperature may exceed the coolant boiling temperature in some regions, possibly resulting in nucleate boiling. Use of correlations that consider only liquids would thus involve significant errors [13]. To take this into account, the effects of nucleate boiling were integrated in the model using Kandlikar's correlation [14]. The correlation was used in the regions where the liner temperature exceeded the coolant boiling temperature, whereas the classical Dittus-Boelter correlation was used elsewhere. In this case the temperature distribution in the liner was assumed to be a 3rd order polynomial (eq. 10) of the normalized height of the liner, h , whose coefficients γ_1, γ_2 and γ_3 were fitted to the experimental data (from [15]) of an engine running in fully warmed up condition (figure 6):

$$T_l(h) = T_l(0) + \left(T_l(h_l) - T_l(0)\right)\left(\gamma_1 \cdot h^3 + \gamma_2 \cdot h^2 + \gamma_3 \cdot h\right) \qquad (10)$$
$$0 \le h \le h_l$$

In equation (16) $T_l(0)$ and $T_l(h_l)$ are the liner temperatures at the bottom and top of the liner, respectively. A generic engine thermal condition can be described by adapting the pairs of $T_l(0)$ and $T_l(h_l)$ temperature values to the actual mean liner temperature T_w , as shown in figure 7, which reports the temperature distributions calculated with equation (10) for liner mean temperatures ranging from cold start to fully warmed up conditions.

Once the temperature distribution in the liner is known, it is possible to determine the height at which the coolant boiling temperature is reached, h_{eboil} (shown graphically in figure 4). The zone of the liner above h_{eboil} is the one affected by nucleate boiling, whereas only forced convection should occur below it.
The heat transfer coefficients for the two zones, α_1 and α_2 , were calculated using the Dittus-Boelter and the Kandlikar correlations, respectively (eqs. A. 1 and B. 1 in the appendix), and then surface-weighted to obtain the mean heat transfer coefficient for the whole liner α_{wc} :

$$\alpha_{wc} = \alpha_1 \frac{h_l - h_{eboil}}{h_l} + \alpha_2 \frac{h_{eboil}}{h_l} \qquad (11)$$

3.2.2. External cooling system

The external cooling system consists of the pump, radiator, thermostatic valve and external connection pipes.
The coolant mass flow $\dot{m}_c$ was obtained from the characteristic curves of the pump and the cooling circuit.
The thermostatic valve behaves as a proportional temperature controller, with a non-linear static gain; the valve time constant is approximately 30 seconds [7]. As the coolant temperature at the engine outlet T_{c,e_out} increases, the thermostatic valve lets more coolant through the radiator, thus increasing $\dot{m}_r$ and simultaneously reducing the coolant mass flow $\dot{m}_{by}$ in the by-pass circuit.
The normalized thermostatic valve lift l_t changes with T_{c,e_out} , as shown in figure 8.
The coolant mass flow through the radiator at a given temperature was assumed to be proportional to valve lift and was thus calculated as:

$$\dot{m}_r = l_t(T_{c,e\_out}) \cdot \dot{m}_c \qquad (12)$$

In a simplified circuit (figure 9) without a cabin heater, EGR cooler or oil cooler, the by-passed coolant mass flow becomes:

$$\dot{m}_{by} = [1 - l_t(T_{c,e\_out})] \cdot \dot{m}_c \qquad (13)$$

The enthalpy balance for the mass of coolant in the radiator is:

$$\dot{m}_r \cdot c_c \cdot T_{c,e\_out} - \dot{Q}_r - \dot{m}_r \cdot c_c \cdot T_{c,r\_out} = m_{c,r} \cdot c_c \cdot \frac{dT_{c,r\_out}}{dt} \qquad (14)$$

The coolant to air heat transfer rate was calculated by:

$$\dot{Q}_r = \alpha_r \cdot A_r \cdot \left(\frac{T_{c,e\_out} + T_{c,e\_in}}{2} - T_a \right) \quad (15)$$

For any given radiator arrangement, the heat transfer coefficient, α_r, increases with air velocity, hence with vehicle speed, v_a, which can be calculated from the engine angular speed, ω_e, the tyre rolling circumference, Γ_t, and the engine to wheel transmission ratio, τ:

$$v_a = \Gamma_t \frac{\omega_e}{2\pi\tau} \quad (16)$$

Tables from [16] allow a good estimation of α_r as a function of v_a for typical automotive applications.

3.2.3 Pump inlet

The mass flow of coolant from the by-pass circuit and the mass flow of coolant from the radiator mix at the pump inlet. Since all components except the engine and the radiator are assumed to be adiabatic, the coolant temperature in the pump does not change, and the same temperature is found both at the pump outlet and at the engine inlet. The latter can therefore be calculated by solving the enthalpy balance at the pump inlet:

$$T_{c,e\_in} = \frac{\dot{m}_{by} \cdot c_c \cdot T_{c,e\_out} + \dot{m}_r \cdot c_c \cdot T_{c,r\_out}}{\dot{m}_c \cdot c_c} \quad (17)$$

4. DETERMINATION OF VEHICLE FUEL CONSUMPTION

After simulating the engine and its cooling system using the approach described in the previous section, we simulated a vehicle equipped with them running on standard cycles. Then, simulations of the same vehicle equipped with the perfect cooling system were run to identify its benefits in terms of fuel consumption.
The block diagram of the simulator used is shown in figure 10. The specifications of a high-medium class passenger car were entered: mass, 1500 kg; frontal area, 2.6 m^2, drag resistance coefficient, 2.8, and a five-speed gearbox.
The engine torque and rotational speed required to run the test cycles were calculated and entered into the engine maps to obtain for each instant:

- the heat transfer rate between combustion chamber and liner
- engine-specific fuel consumption

Since these depend on the engine thermal conditions, the external engine cooling system model was also solved by using equations 1 to 17 to obtain the relevant temperatures of engine components, coolant and oil.
Knowledge of the fuel consumption values in the selected cycle and of the distance travelled allowed calculation of the amount of fuel needed to travel 100 km.

5. RESULTS AND DISCUSSION

This section reports a selection of the results obtained using the proposed simulator.
First of all the vehicle's behaviour with the conventional cooling system is described by the aid of figure 11, which shows vehicle velocity, liner temperature, coolant temperature at the engine inlet and outlet, oil temperature, thermostatic valve position and engine fuel consumption for the NEDC.
Since the cycle starts with a cold engine, the first step of the simulation involves only ambient temperatures. As the engine warms up the liner temperature rises and coolant temperatures at the engine outlet and inlet grow almost simultaneously. Then, when the engine outlet temperature has reached about 60 °C, the thermostatic valve begins to open, and some of the coolant flows through the radiator, where it is cooled. From this point on, the engine inlet temperature is lower than that at the engine outlet. The position of the thermostatic valve changes according to the behaviour of its wax temperature-sensitive part. The oil temperature, which in the model is assumed to be equal to that of the engine block, behaves like the liner and the coolant temperature, its mean value rising with cycle time but much more slowly, due to its greater mass and greater thermal inertia.
The effect of smart thermal management is then demonstrated by comparing the results from the conventional cooling system to those obtained using the 'perfect' cooling system, defined in section 2. This is done in figure 12, where two different perfect cases are compared to the standard case using the NEDC. Case 1 is a vehicle equipped with a cooling system that can warm up the engine instantly and maintain a constant set point temperature (this system fulfils principles #1, #2 and #3 of section 2. Case 2 applies the more realistic principle #3a instead of #3: the engine is adiabatic during the warm-up phase, i.e. the heat fluxes to the ambient through the engine block and the coolant are assumed to be zero; when the temperature set point is reached the cooling system converges with the one modelled in case 1.

As shown in figure 12, the liner temperature set point, which is assumed to be the maximum allowable mean liner temperature, is reached immediately in case 1, it is reached in about 300 seconds in case 2, and is not reached at all with the conventional system.
The delay in reaching the fully warmed up condition and/or the imperfect control of the engine thermal status involve significantly greater friction losses, as shown in figure 13, where the *FMEP* (calculated by eq. 9) for Case 2 and for the conventional cooling system are compared for the NEDC normalized cycle. Figure 14 shows the heat generated per unit time that is associated with these friction losses.
Figure 14 compares the conventional and the perfect cooling system (Case 2) in terms of heat flow rate transferred from the in cylinder gases to the walls during the NEDC cycle; with the conventional cooling system more heat than necessary is transferred to the walls, increasing the thermal losses.
Figure 14 also shows the heat transferred to the ambient per unit time by the engine with the conventional cooling system, something that in the perfect cooling system is prevented from happening.
The conventional cooling system involves significantly greater fuel consumption, as shown in table 2, where Case 1, Case 2, and the conventional cooling system are compared for the NEDC, the EU CITY, and the most common US and Japanese normalized cycles.
Savings are greatest in the cycles simulating urban conditions, where engine loads are lowest. In such conditions an improved thermal management system offers the greatest advantages, whereas a conventional system is associated with mean engine temperatures that are well under fully warmed up values, excessively low oil temperature, and greater friction.

6. CONCLUSIONS

A method to evaluate the effects of an improved engine thermal management system for a passenger car is proposed.
A 'perfect' cooling system was simulated and its effects on the engine thermal status defined with a view to establishing a reference to which different cooling and control system concepts could be compared.
A conventional cooling system was then compared to the 'perfect' cooling system to estimate the fuel economy that can be achieved through the adoption of thermal management in a passenger car run on standard driving cycles.
Two different cases were hypothesized for the 'perfect' cooling system: a system that warms up the engine instantly and maintains its set point temperature constant, and a more realistic case where the engine is assumed to be adiabatic while warming up. When the temperature set point is reached the two cases converge, because the cooling system is again assumed to be able to maintain its set point temperature constant.
The data required for the engine thermal modelling were obtained from a preliminary analysis using the AVL Boost program. Models for all the components of the power train and cooling system were developed and linked to simulate an upper-medium segment passenger car, which was then run on standard cycles. The use of a perfect system means that the simulated fuel consumption reductions constitute theoretical maxima for this car.
The results showed that delays in reaching the fully warmed-up condition and/or imperfect control of the engine thermal status both influence fuel consumption. Greater advantages were found in the cycles simulating urban conditions, where engine loads are lowest. These are the conditions in which an improved thermal management system offers the greatest gains, whereas in a conventional cooling system the mean engine temperatures are well under fully warmed up values, oil temperature is excessively low, and friction is greater.
Possible directions for research continuation include the collection of experimental data to verify the results of the simulation as well as result generalization by extending the data to different classes of cars.

APPENDIX

A. Dittus-Boelter correlation

The Dittus-Boelter correlation [12] calculates the heat transfer coefficient in horizontal tubes, $\overline{\alpha_c}$, as:

$$\overline{\alpha_c} = 0.023 \cdot Re^{0.8} \cdot Pr^{0.4} \cdot \left(\frac{\lambda_c}{D_e} \right) \qquad \text{(A. 1)}$$

where:

λ_c thermal conductivity of the coolant ($W\,m^{-1}\,K^{-1}$)

D_e equivalent diameter of the engine coolant path around the liner *(m)*

In the paper this correlation is used to calculate the coolant to wall heat transfer flux. The Reynolds number, *Re*, and Prandtl's number, *Pr*, of the coolant are calculated based on cooling pump flow rate, cooling path section around the liner, and coolant mean temperature.

B. Kandlikar correlation

This correlation has been proposed to evaluate the heat transfer coefficient in horizontal tubes, $\overline{\alpha_{tp}}$, where nucleate boiling occurs [14]:

$$\frac{\overline{\alpha_{tp}}}{\alpha_c} = C_1 \cdot Co^{C_2} \cdot (25 \cdot Fr)^{C_5} + C_3 \cdot Bo^{C_4} \qquad \text{(B. 1)}$$

where:

$Bo = \frac{q}{G \cdot i_{ig}}$ boiling number

q coolant heat flux ($W\ m^{-2}$)

G specific mass flow ($kg\ s^{-1}\ m^{-2}$)

i_{ig} latent heat of vaporization ($J\ kg^{-1}$)

$Co = \left(\frac{1-x}{x}\right)^{0.8} \cdot \left(\frac{\rho_g}{\rho_l}\right)^{0.5}$ convection number

x dryness fraction (-)

ρ_g vapour density ($kg\ m^{-3}$)

ρ_l liquid density ($kg\ m^{-3}$)

$Fr = \frac{G^2}{\rho_l^2 \cdot g \cdot L}$ Froude number (-)

g gravity acceleration ($m\ s^{-2}$)

The value of *Co* divides the whole surface in two regions:

Co<0.65 convective boiling region (convective mechanism)

Co>0.65 nucleate boiling region (nucleate boiling mechanism)

The values of constants C_1 - C_5 are reported in table 3.

In any given condition the heat transfer coefficient, $\overline{\alpha_{tp}}$, is obtained using the two sets of constants for the two regions.

Since the transition from one region to the other occurs at the intersection of the respective correlations, the higher transfer coefficient value is the predicted value of the proposed correlation.

The Kandlikar correlation is used in the paper to calculate the coolant to wall heat transfer flux in the region where the engine liner walls reach temperatures that exceed the coolant boiling temperature.

The dryness fraction, *x*, is assumed to be proportional to the difference between mean liner temperature and coolant boiling temperature.

ACKNOWLEDGEMENTS

The authors are grateful to Dr. Silvia Modena for the language review

REFERENCES

[1] P. Setlur, J.R. Wagner, D.M. Dawson and E. Marotta, An Advanced Engine Thermal Management System: Nonlinear Control and Test, IEEE/ASME Transactions on Mechatronics, Vol. 10, Issue 2, April 2005.

[2] P. Setlur, J. Wagner, D. Dawson and J. Chen, Nonlinear Controller for Automotive Thermal Management Systems, Proceedings of the American Control Conference, June 4-6, 2003, Denver, Colorado.

[3] M. H. Salah, T. H. Mitchell, J. R. Wagner and D. M. Dawson, Nonlinear-Control Strategy for Advanced Vehicle Thermal-Management Systems, IEEE Transactions on Vehicular Technology, Vol. 57, No. 1, January 2008.

[4] N. Staunton, V. Pickert and R. Maughan, Assessment of Advanced Thermal Management Systems for Micro-Hybrid Trucks and Heavy Duty Diesel Vehicles, IEEE Vehicle Power and Propulsion Conference (VPPC), September 3-5, 2008, Harbin, China.

[5] A. J. Torregrosa, A. Broatch, P. Olmeda and C. Romero, Assessment of the influence of different cooling system configurations on engine warm-up, emissions and fuel consumptions, International Journal of Automotive Technology, Vol. 9, No. 4, 2008.

[6] M. H. Salah, P. M. Frick, J. R. Wagner and D. M. Dawson, Hydraulic actuated automotive cooling systems – Nonlinear control and test, Control Engineering Practice 17 (2009) 609–62.
[7] L. Guzzella and C. H. Onder, Introduction to Modeling and Control of Internal Combustion Engine Systems, ISBN 3-540-22274-x, Springer, Berlin Heidelberg New York, 2004.
[8] T. Tumus, B. Maniam, M. Mahajan, G. Anand and N. Jain, e-Thermal: A Vehicle-Level HVAC/PTC Simulation tool, SAE 2004 World Congress & Exhibition, Detroit, USA, March 2004.
[9] B. Luptowski, O. Arici, J. Johnson, and G. Parker, Development of the Enhanced Vehicle and Engine Cooling System Simulation and Application to Active Cooling Control, SAE 2005 World Congress & Exhibition, Detroit, USA, April 2005.
[10] I.K. Yoo, K. Simpson, M. Bell and S. Majkowski, An Engine Coolant Temperature Model and Application for Cooling System Diagnosis, SAE 2000 World Congress, Detroit, USA, March 2000.
[11] J. Eberth, J. Wagner, B. Afshar and R. Foster, Modeling and Validation of Automotive "Smart" Thermal Management System Architectures, SAE 2004 World Congress & Exhibition, Detroit, USA, March 2004.
[12] F. Kreith, Principles of Heat Transfer, ISBN 88-207-0356-4, Donnelly Publishing Corporation, New York, 1973.
[13] J.P. Kroes, C. W. M. van der Geld and E. van Velthooven, Modeling of nucleate boiling in engine cylinder head cooling ducts, proceedings of HEAT 2008, Fifth International Conference on Transport Phenomena In Multiphase Systems, Bialystok, Poland, June 30 - July 3, 2008.
[14] S. G. Kandlikar, A general correlation for saturated two-phase flow boiling heat transfer inside horizontal and vertical tubes, Journal of Heat Transfer Vol. 112/219, 1990.
[15] J. B. Heywood, Internal combustion engine fundamentals, ISBN 0-07-028637-x, McGraw-Hill Book Company, New York, 1988.
[16] G. Ferrari, Motori a Combustione interna, ISBN 88-426-7006-5, Edizioni Il Capitello, Torino, 2001.

Table1

1

Engine configuration	4 cylinders inline
Displacement	2000 cc
Bore	86 mm
Stroke	86 mm

2

Table2

1

Cycle	Conventional cooling system	Perfect cooling system Case 1		Perfect cooling system Case 2	
	Fuel consumption (litres/100 km)	Fuel consumption (litres/100 km)	Fuel consumption reduction (%)	Fuel consumption (litres/100 km)	Fuel consumption reduction (%)
EU CITY (European Urban driving cycle)	12.0	8.6	28	10.6	12
EUDC (Extra-Urban Driving Cycle)	7.4	6.6	11	6.8	8
NEDC (New European Driving Cycle)	8.8	7.3	17	7.6	14
USA FTP 75 (USA Federal Test Procedure 75)	7.6	6.8	11	7.1	7
USA FTP Highway (USA Federal Test Procedure Highway)	6.3	5.8	8	5.9	6
Japan 10 Mode (Japanese urban driving cycle)	11.9	9.0	24	11.2	6
Japan 10-15 Mode (Japanese urban and extra-urban driving cycle)	9.3	7.7	17	8.2	12

2

Table3

1

Constant	Convective region	Nucleate boiling region
C_1	1.136	0.6683
C_2	-0.9	-0.2
C_3	667.2	1058
C_4	0.7	0.7
C_5	0.3	0.3

2

Figure1

Click here to download high resolution image

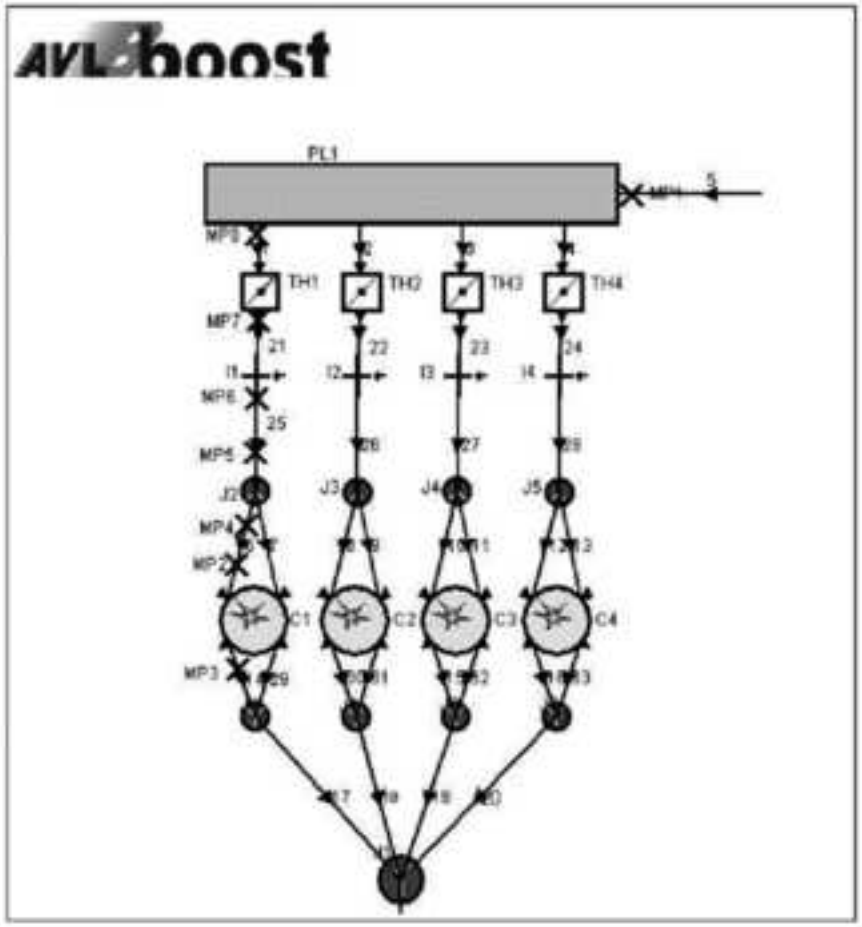

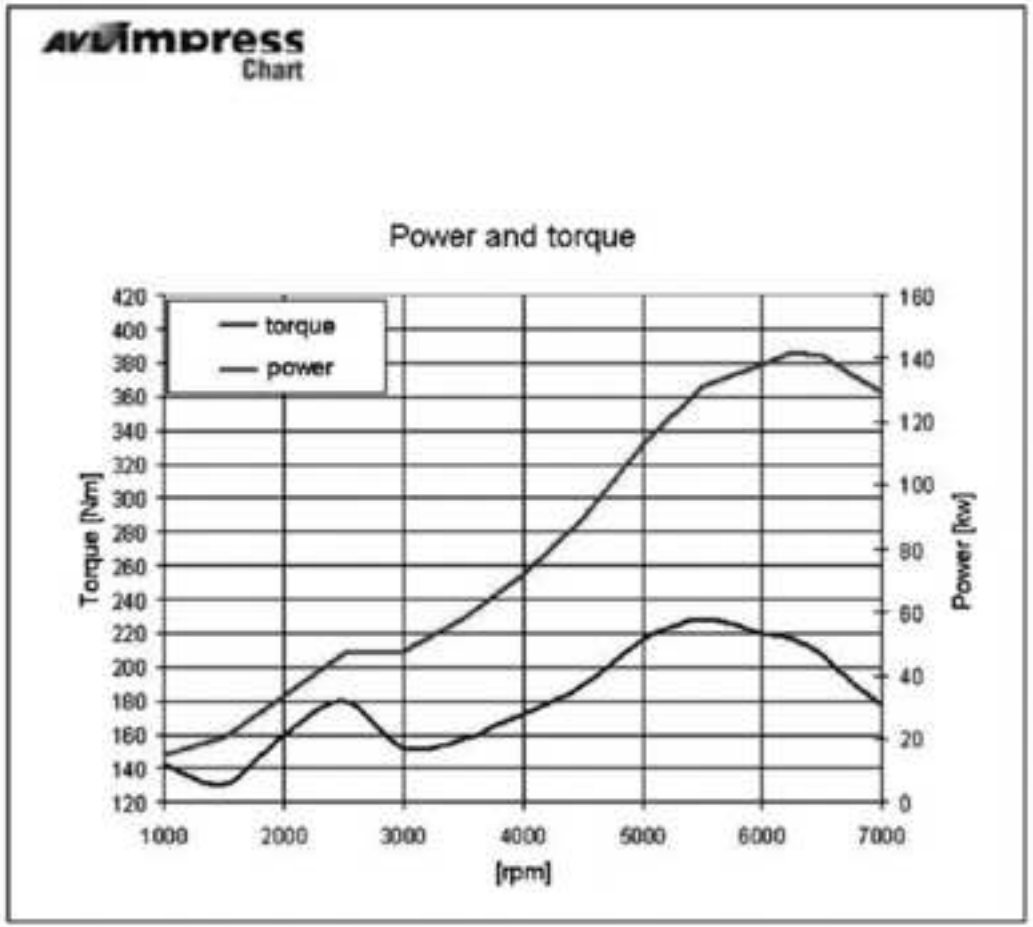

Figure2

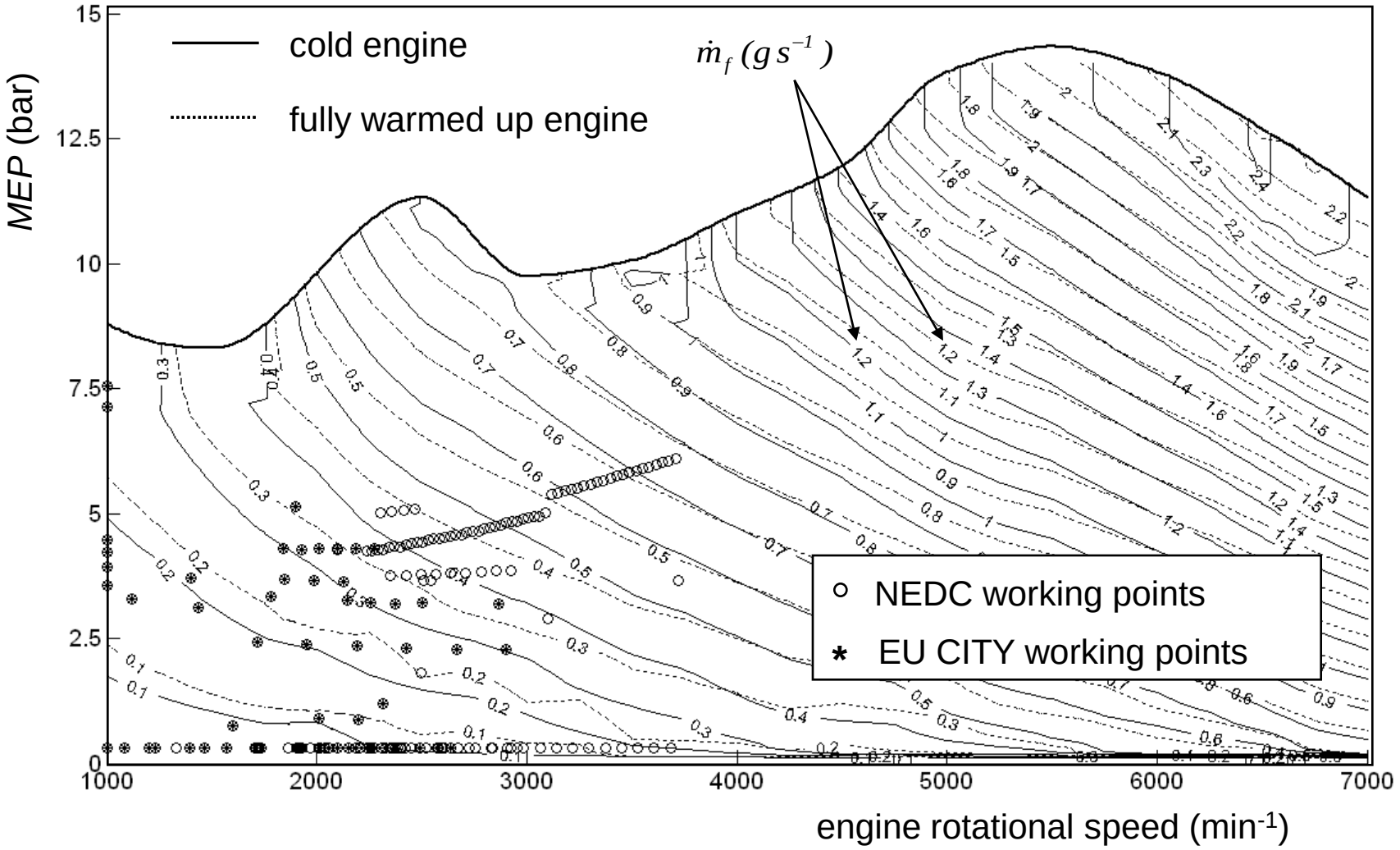
cold engine
fully warmed up engine
$\dot{m}_f\,(g\,s^{-1})$
NEDC working points
EU CITY working points
MEP (bar)
engine rotational speed (min-1)
15
12.5
10
7.5
5
2.5
0
1000
2000
3000
4000
5000
6000
7000

Figure3

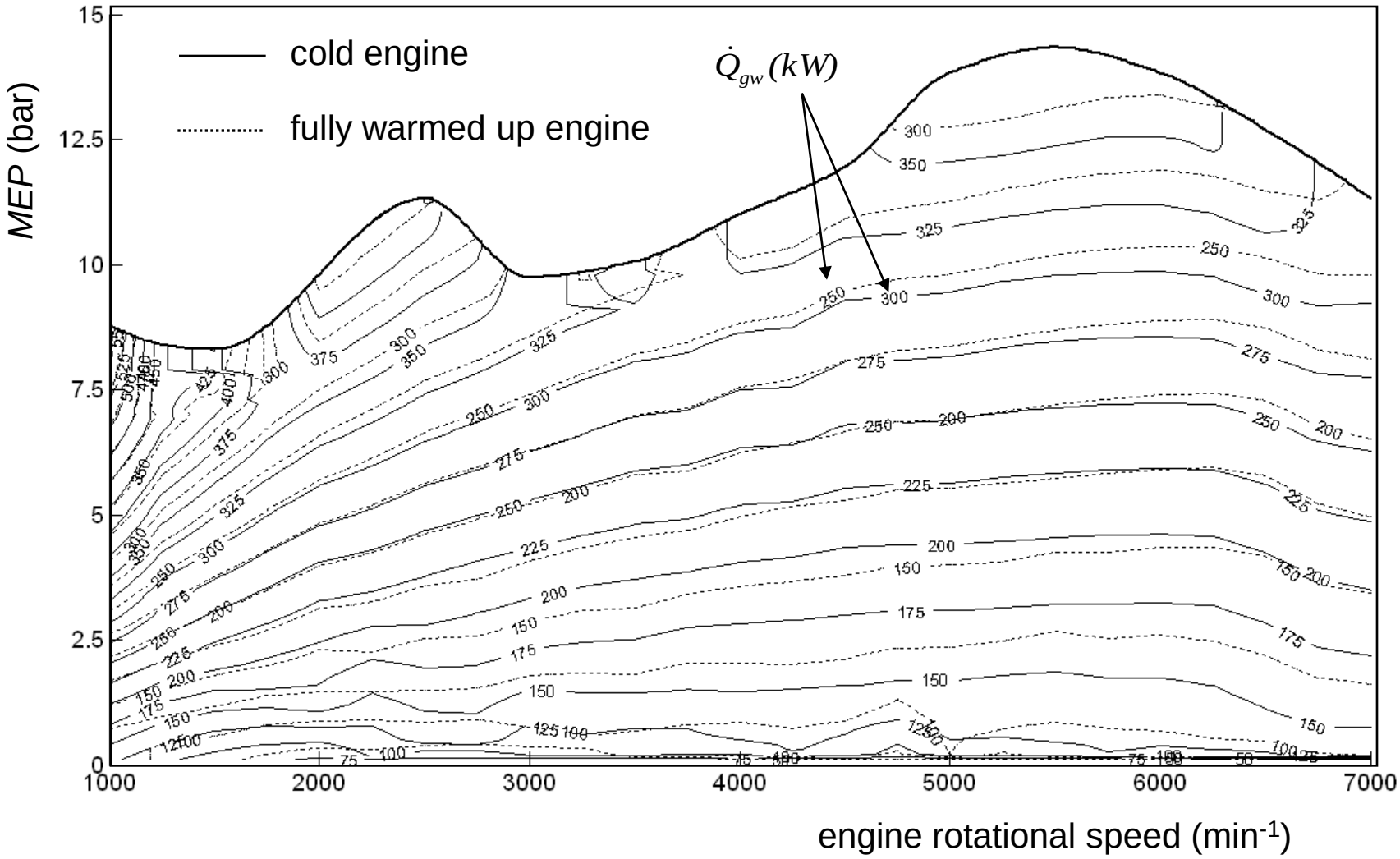
cold engine
fully warmed up engine
$\dot{Q}_{gw}\,(kW)$
MEP (bar)
engine rotational speed (min-1)
0
2.5
5
7.5
10
12.5
15
1000
2000
3000
4000
5000
6000
7000

Figure4

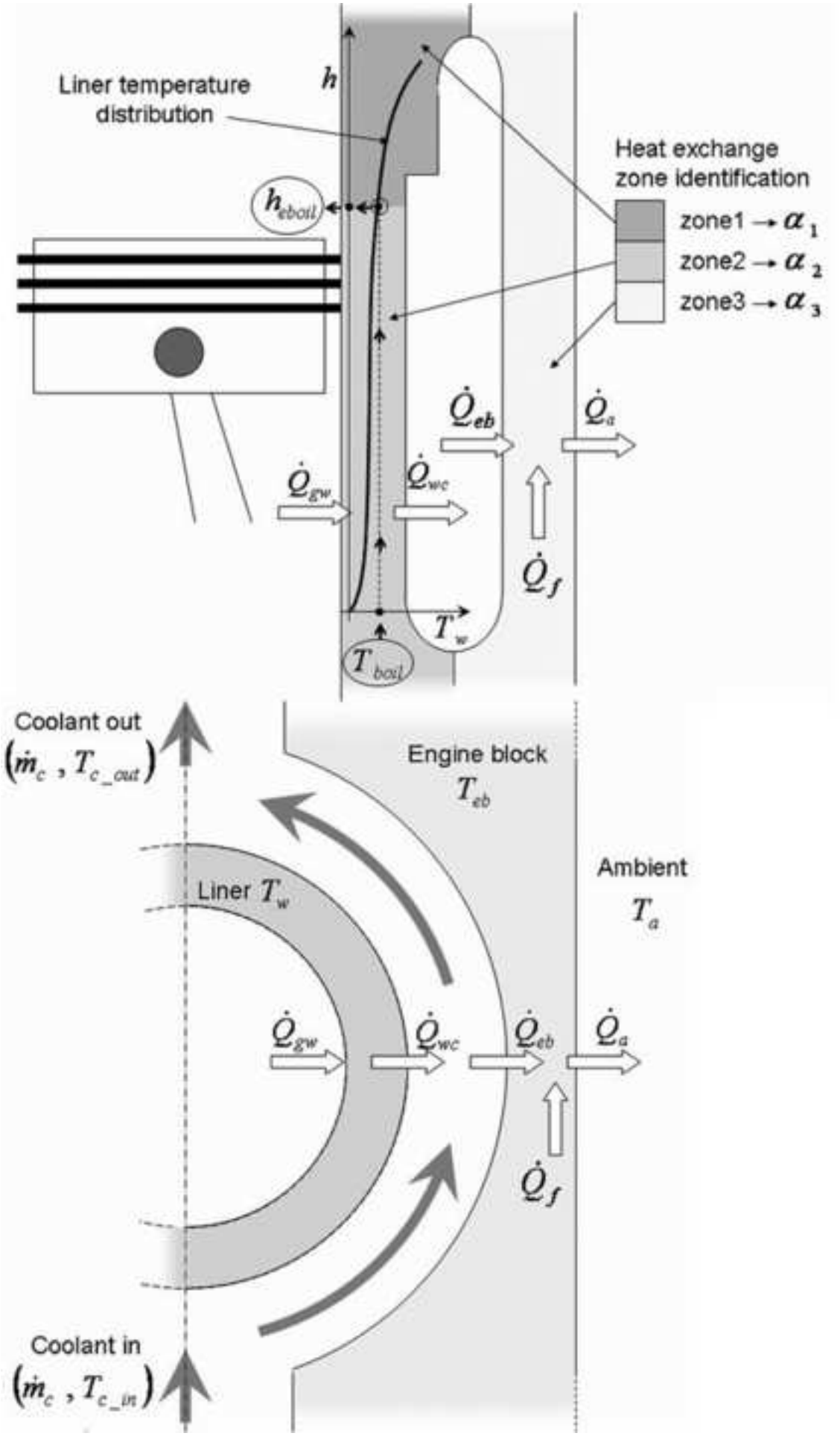

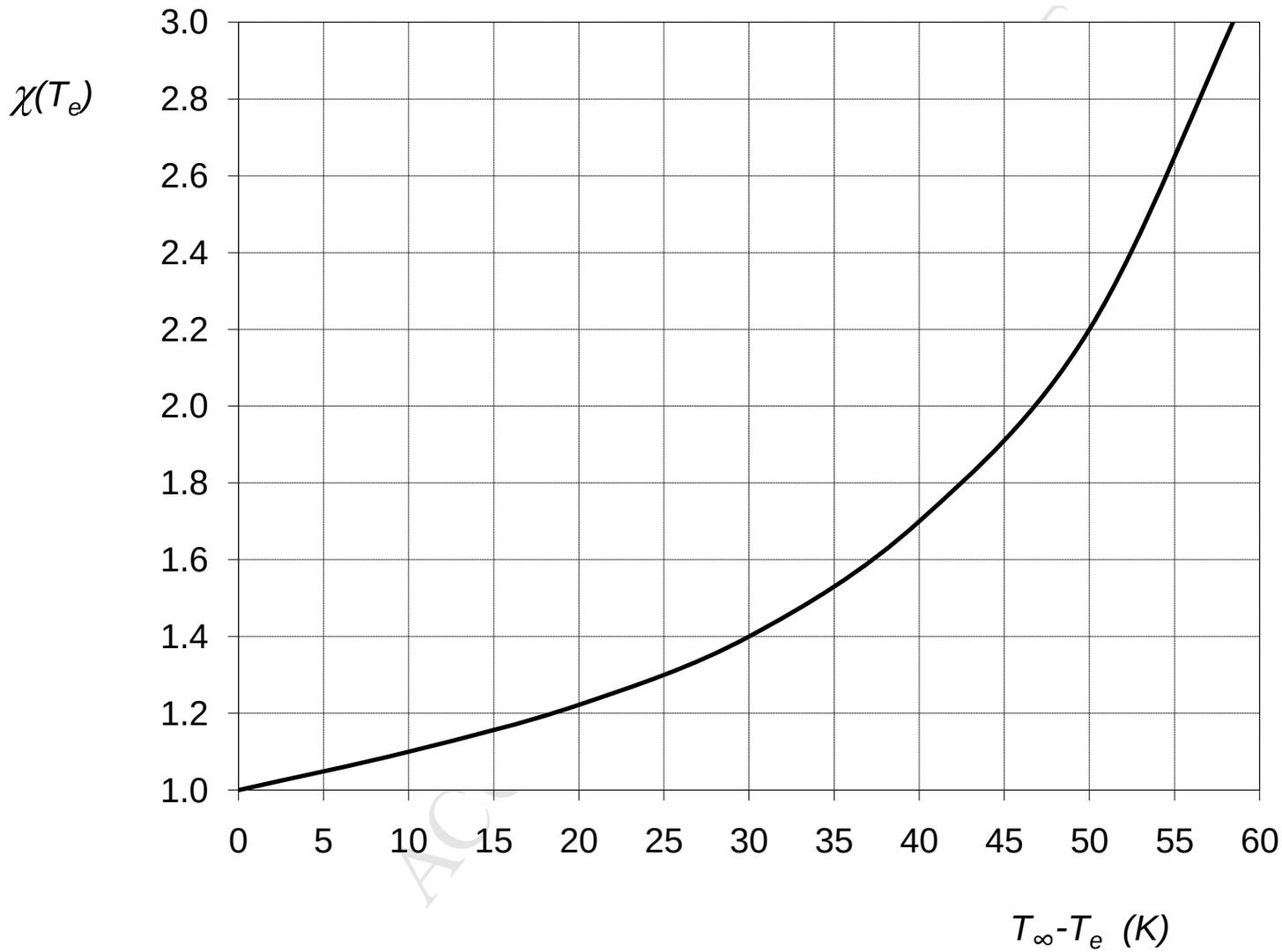

Figure6

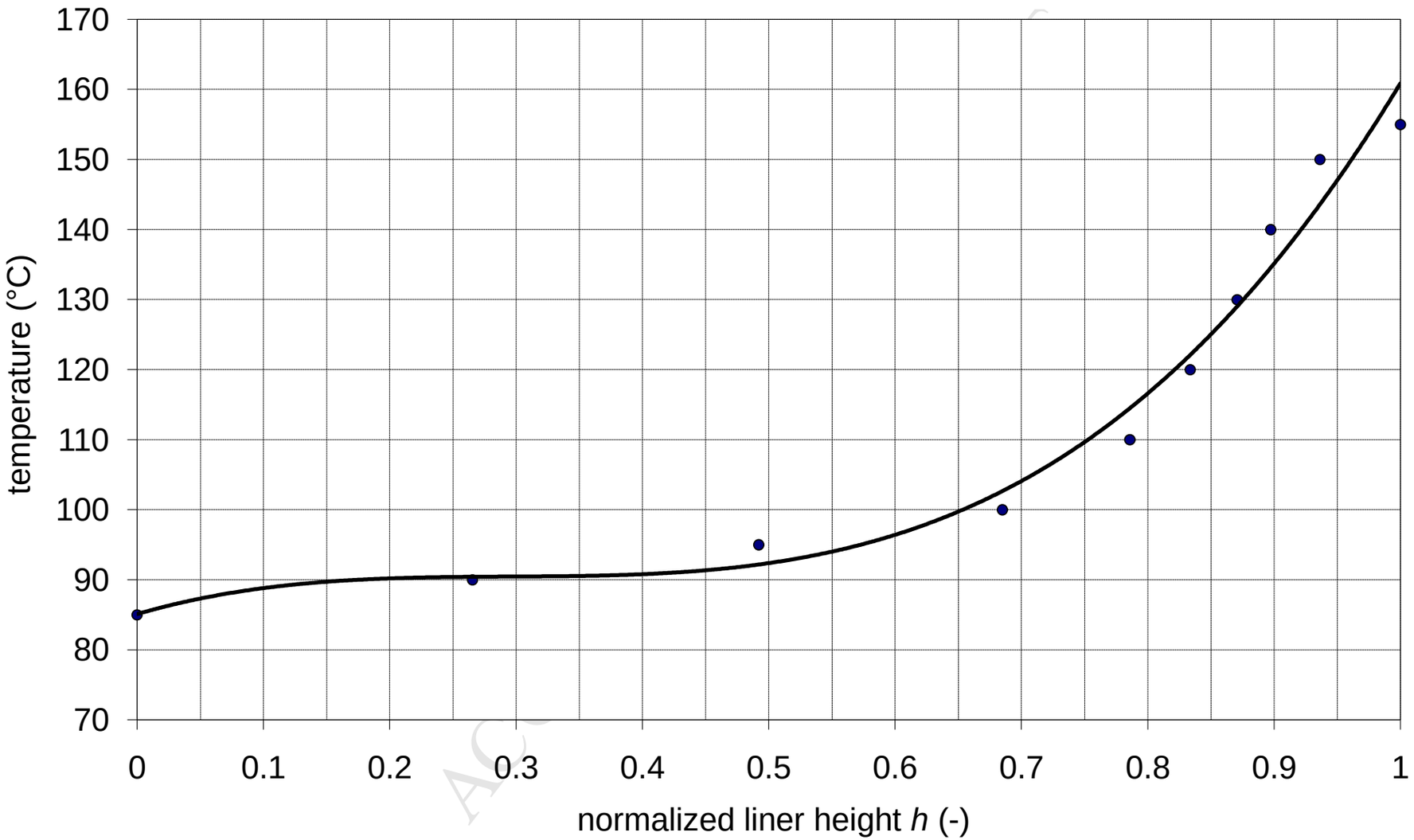

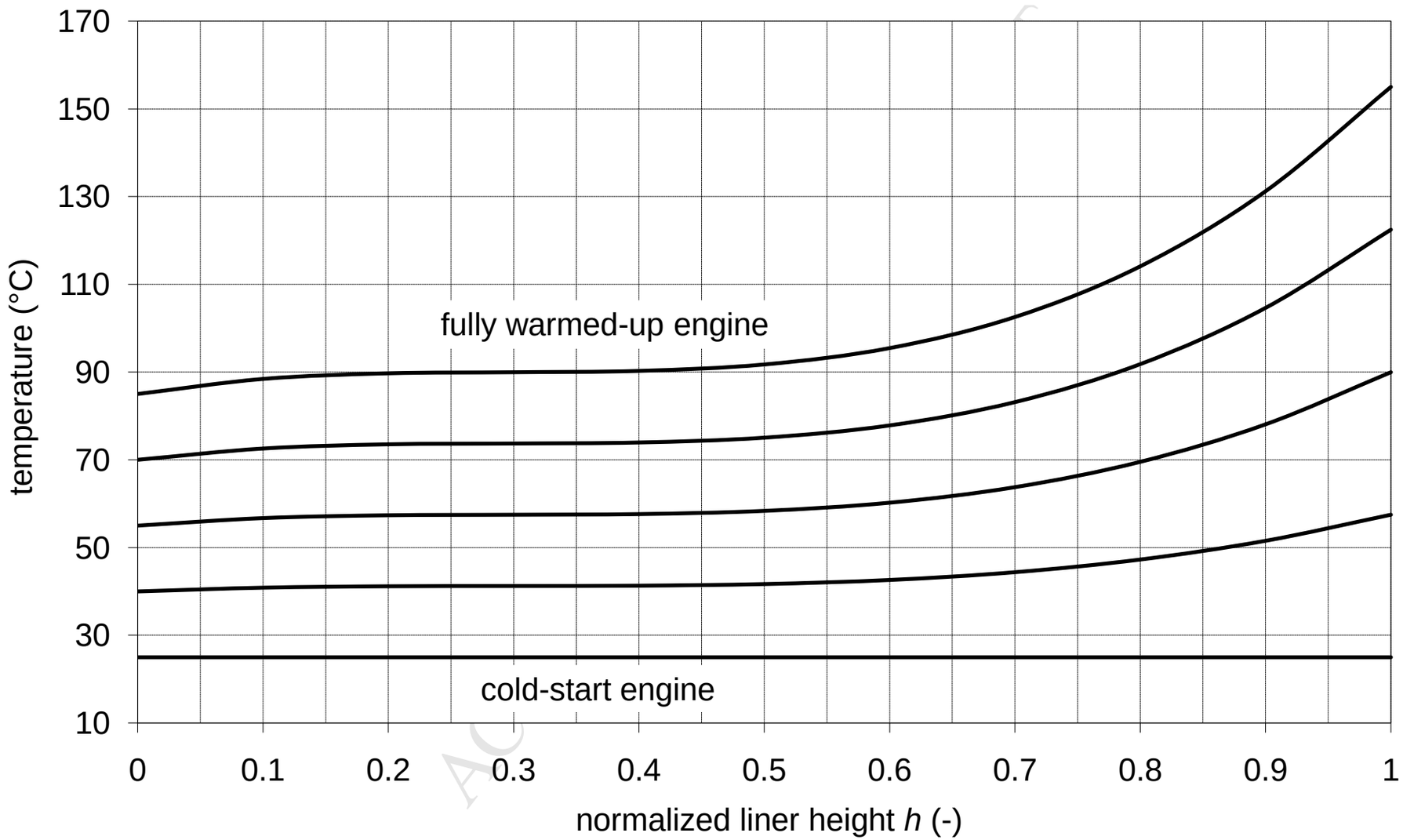

Figure8

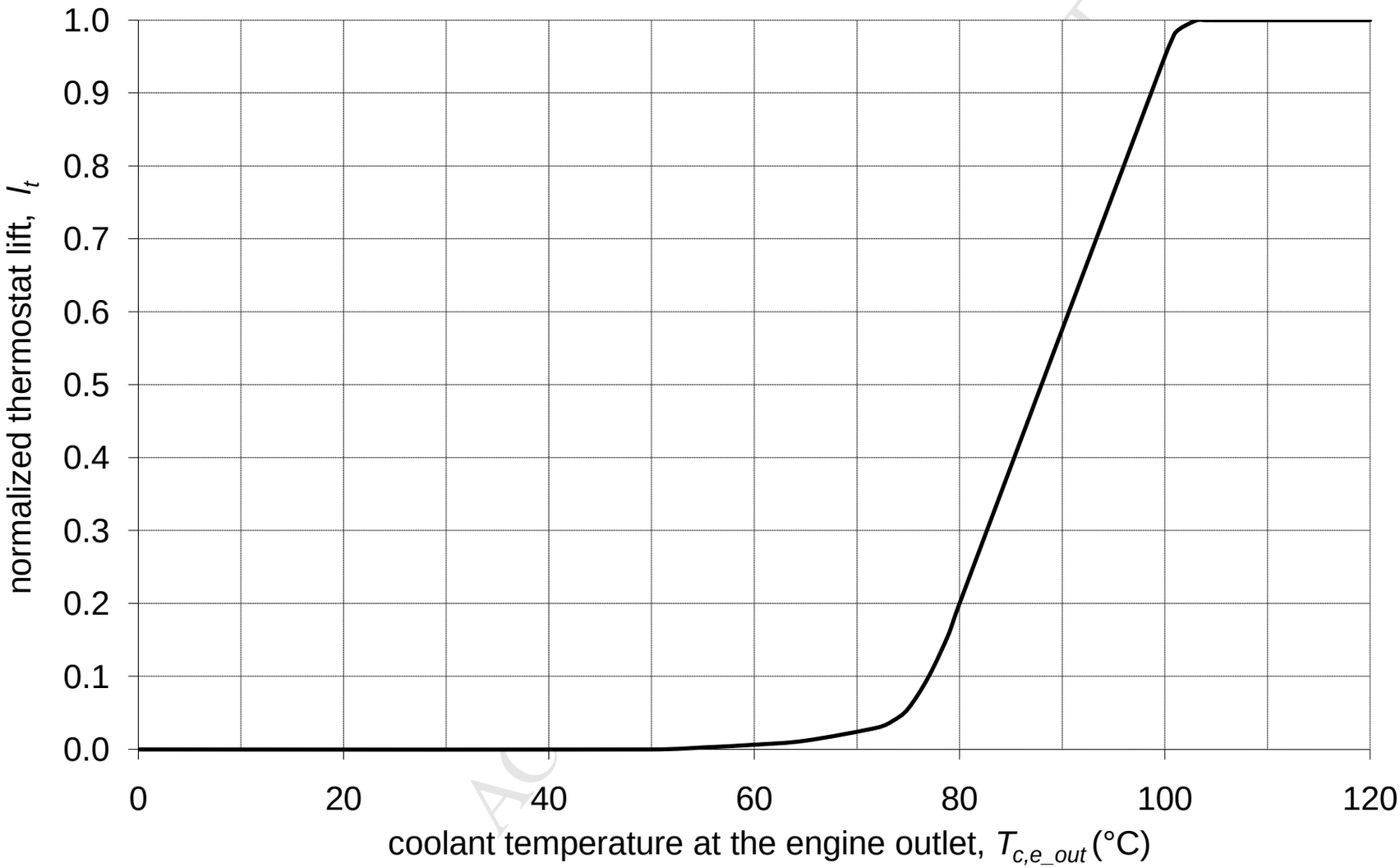

Figure9

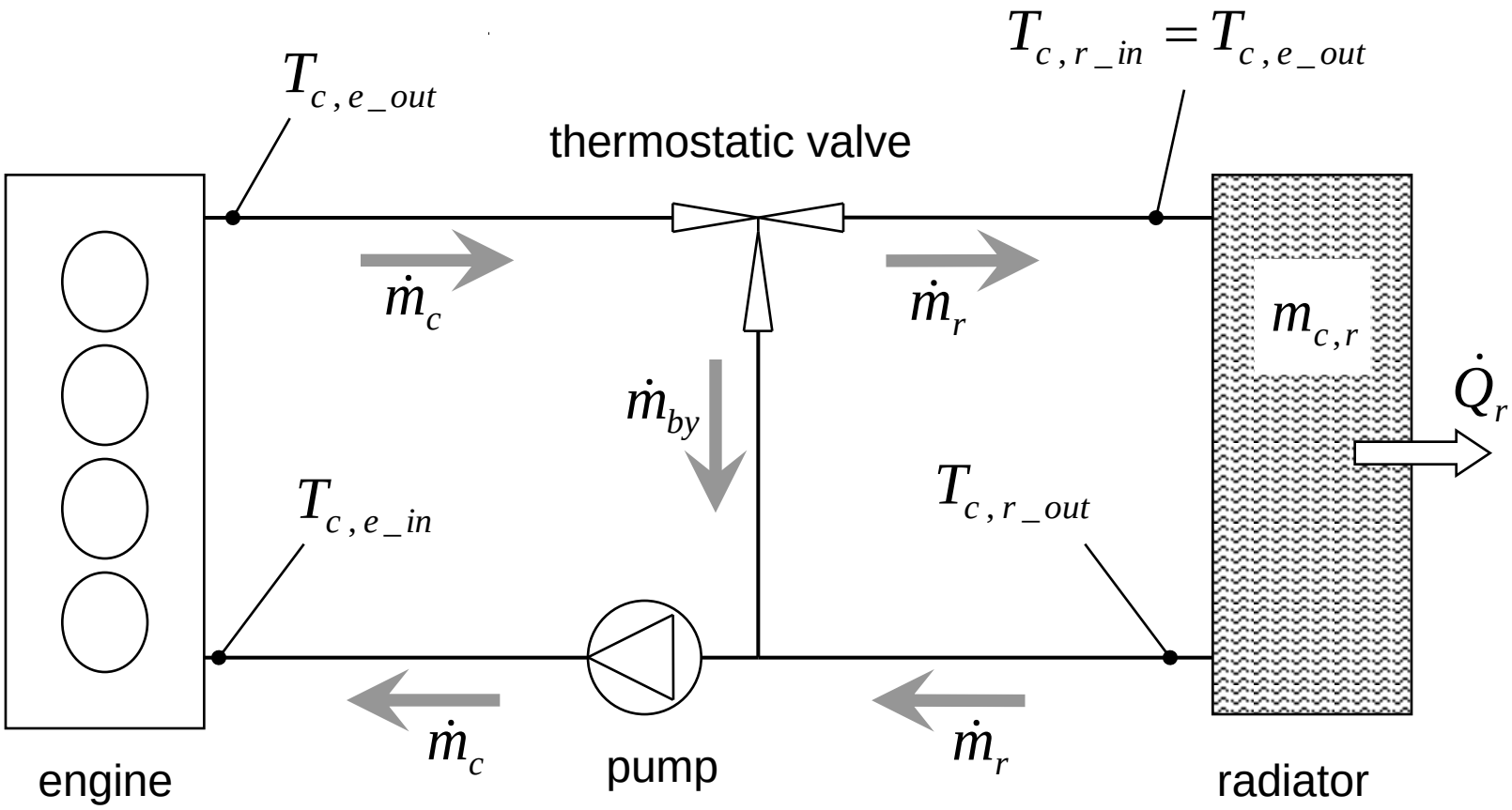
T_{c,e_out}
$T_{c,r\_in} = T_{c,e\_out}$
thermostatic valve
$\dot{m}_c$
$\dot{m}_r$
$m_{c,r}$
$\dot{Q}_r$
$\dot{m}_{by}$
T_{c,e_in}
T_{c,r_out}
$\dot{m}_c$
$\dot{m}_r$
engine
pump
radiator

Figure10

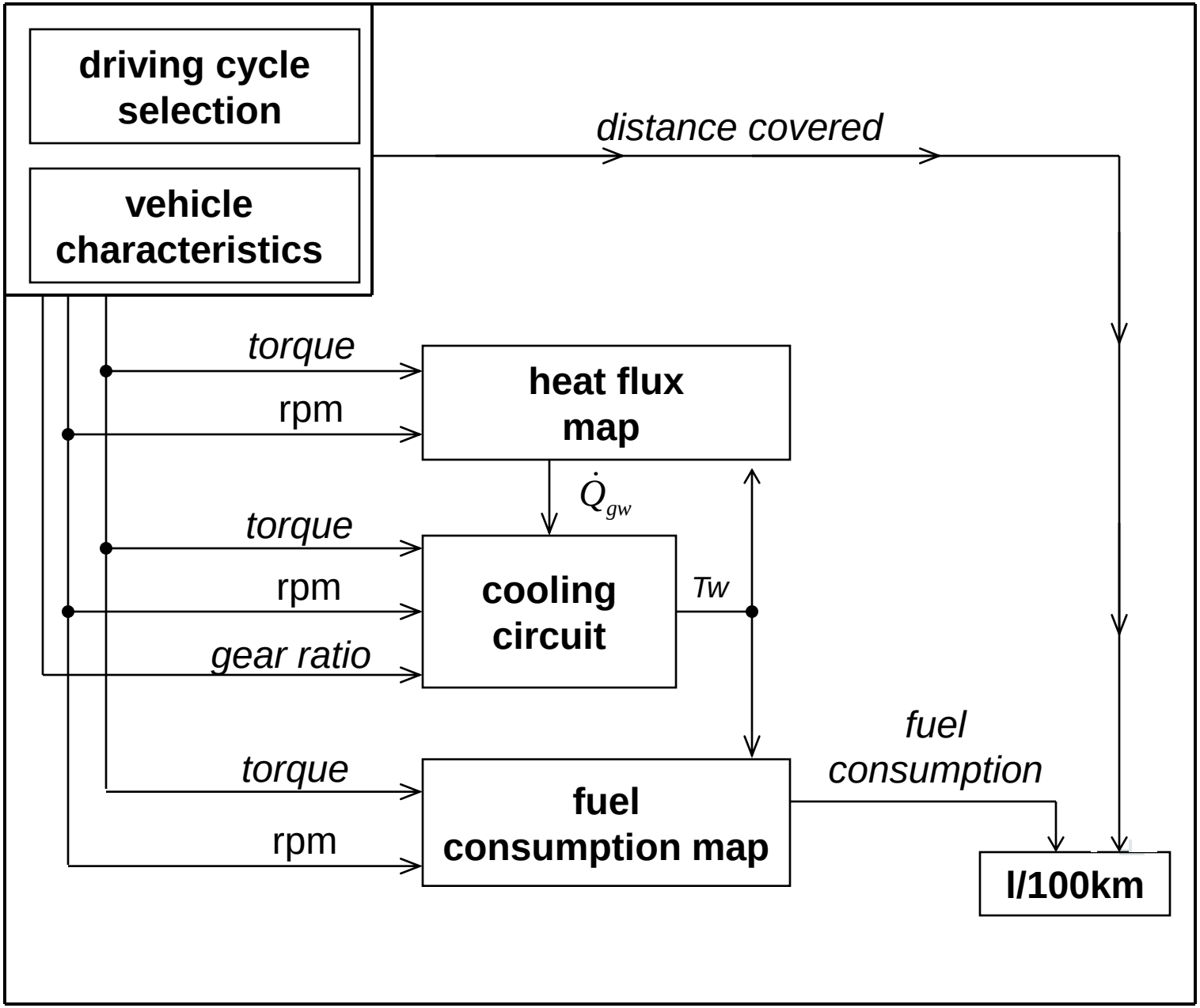
driving cycle selection
vehicle characteristics
distance covered
torque
rpm
heat flux map
$\dot{Q}_{gw}$
torque
rpm
gear ratio
cooling circuit
Tw
torque
rpm
fuel consumption map
fuel consumption
l/100km

Figure11

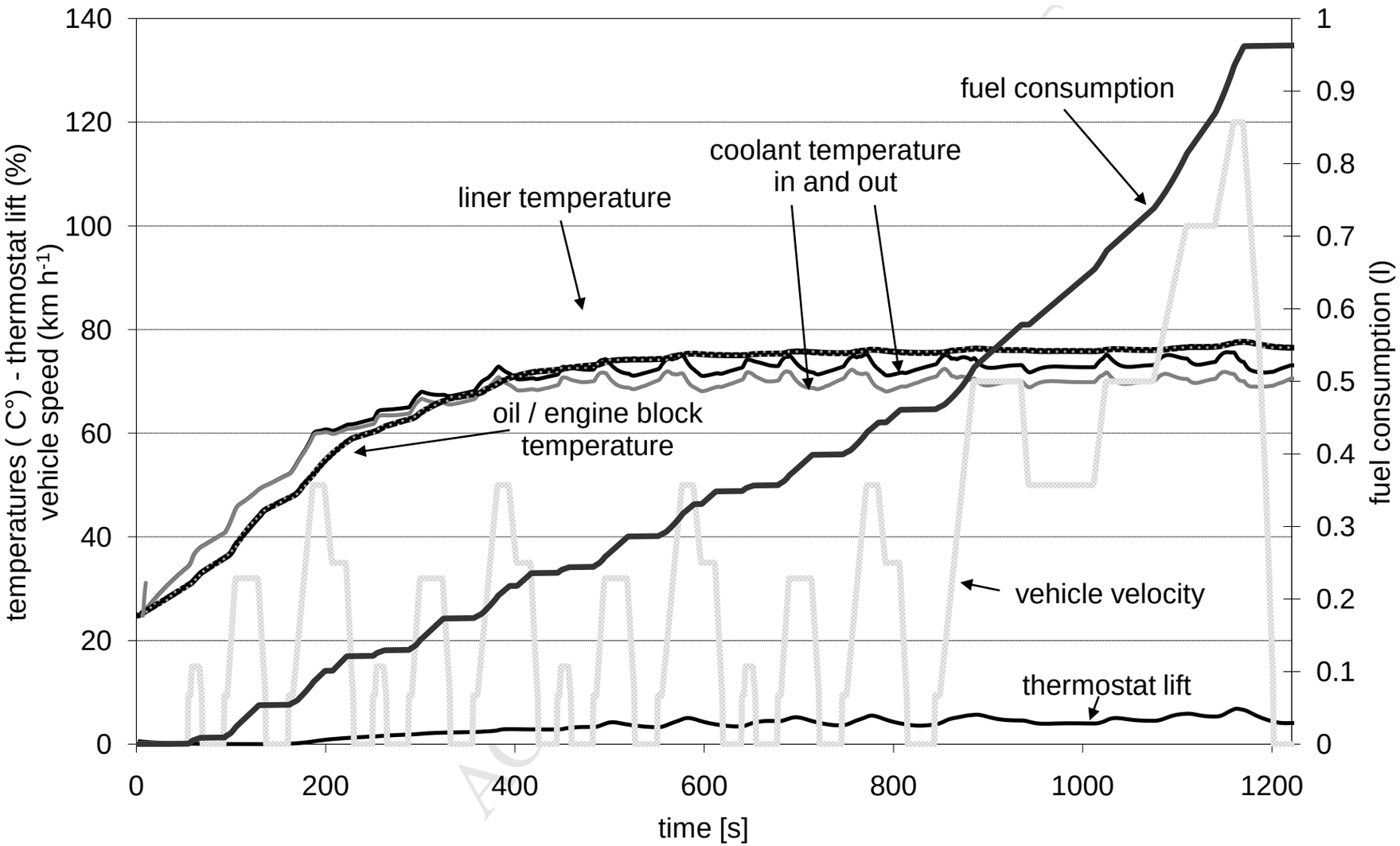

Figure12

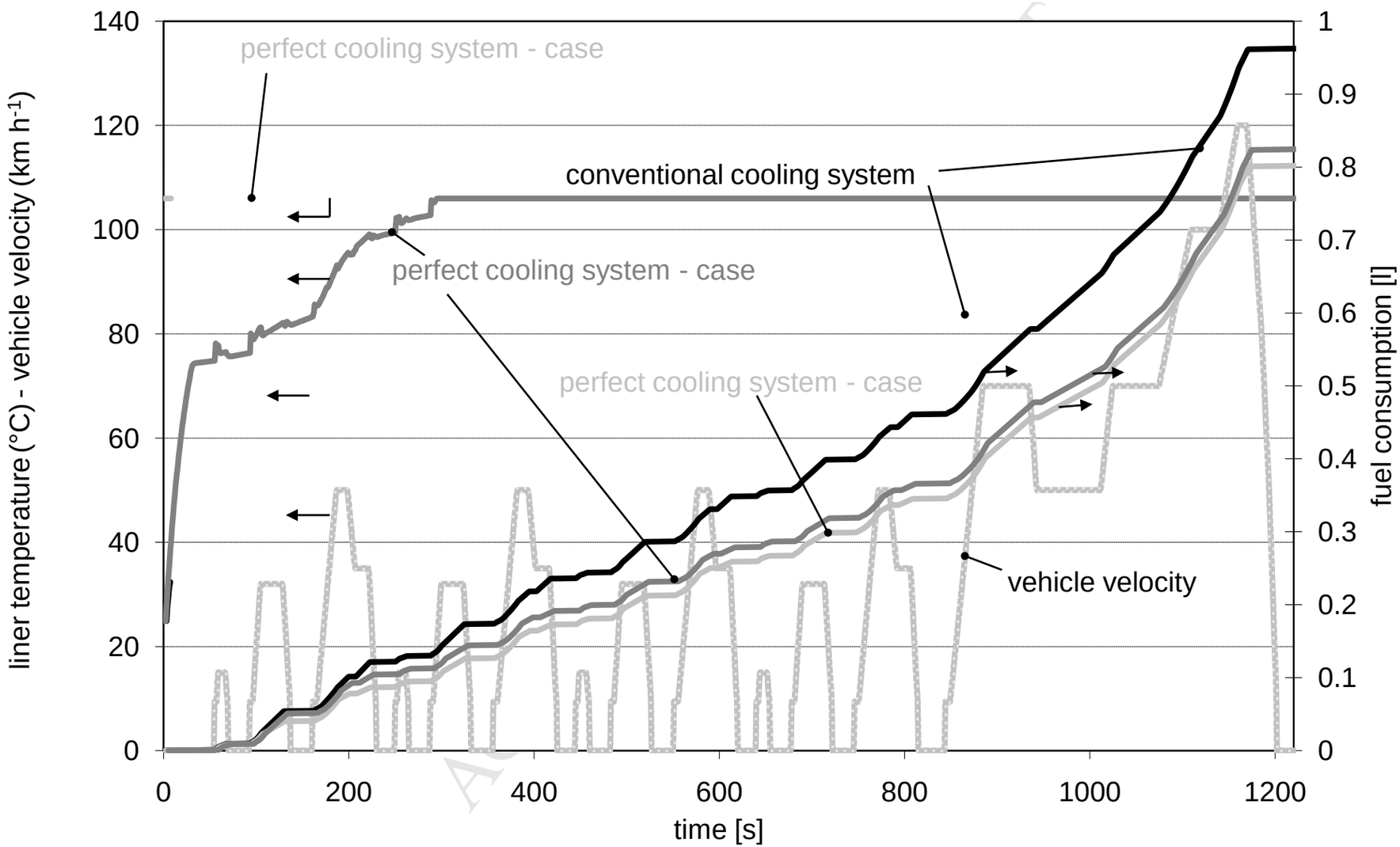

Figure13

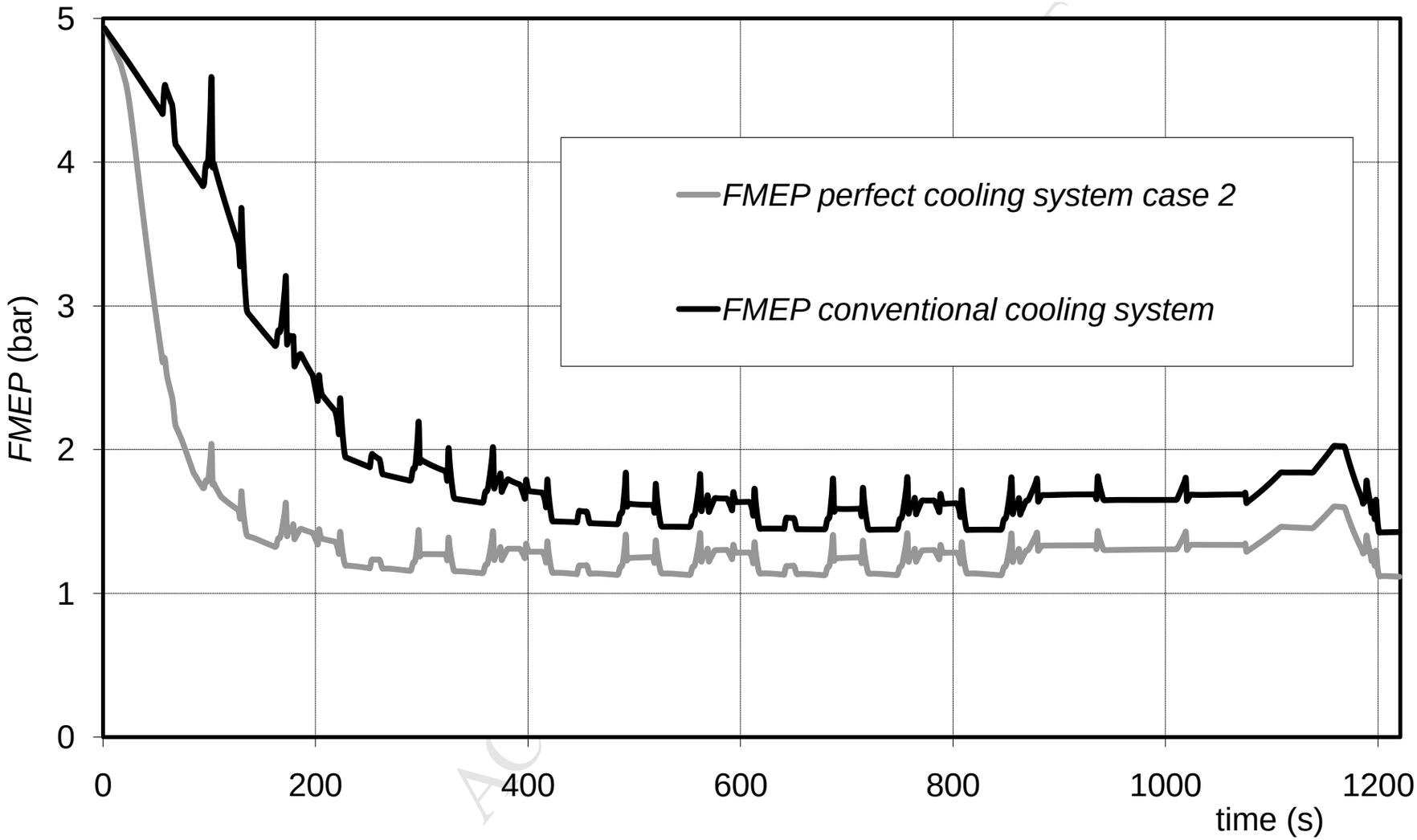

Figure14

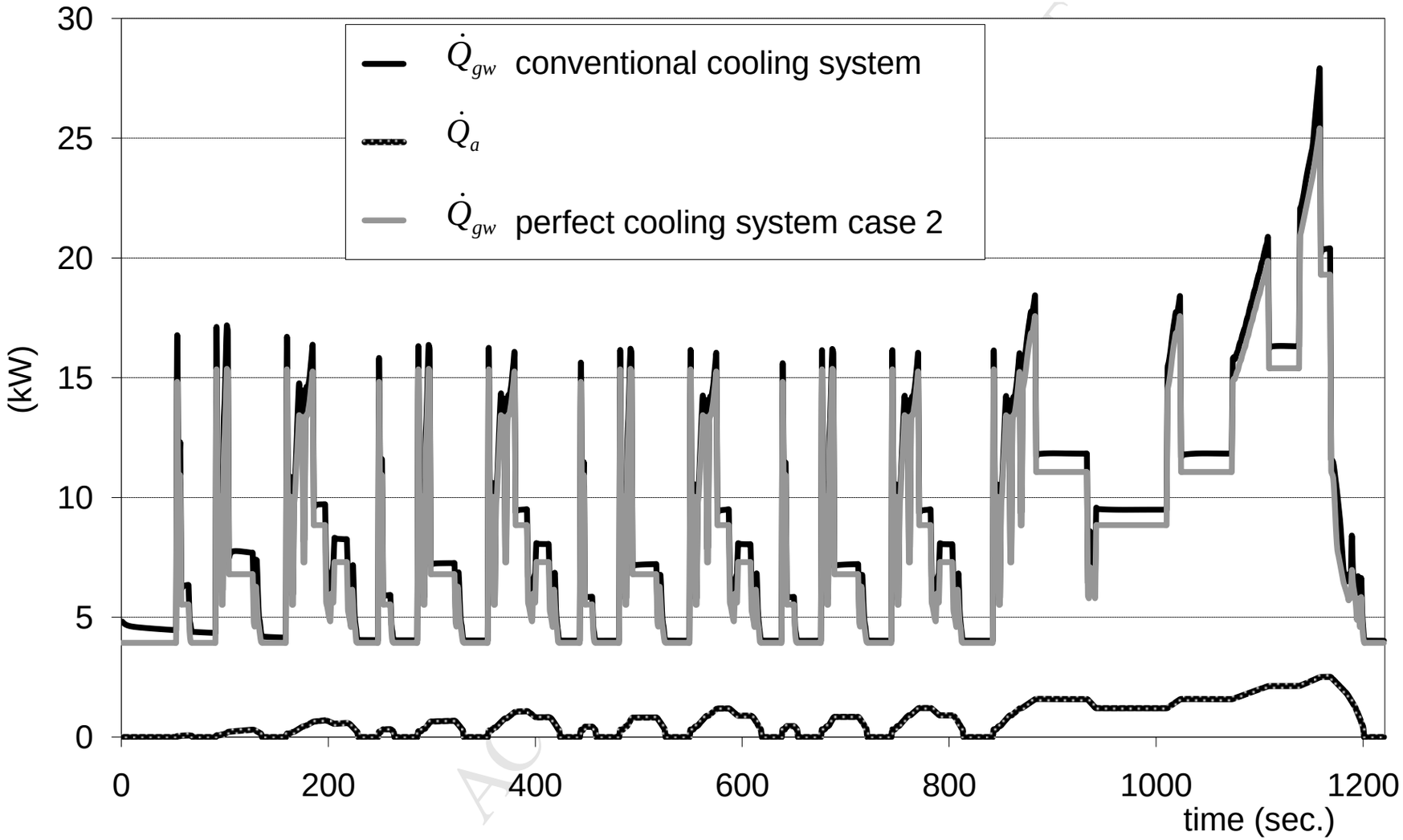

FIGURES

TABLES